Quantitative InfraRed Thermography Journal

ISSN: 1768-6733 (Print) 2116-7176 (Online) Journal homepage: https://www.tandfonline.com/loi/tqrt20

Method of classification of global machine conditions based on spectral features of infrared images and classifiers fusion

Marek Fidali & Wojciech Jamrozik

To cite this article: Marek Fidali & Wojciech Jamrozik (2019) Method of classification of global machine conditions based on spectral features of infrared images and classifiers fusion, Quantitative InfraRed Thermography Journal, 16:1, 129-145, DOI: 10.1080/17686733.2018.1557453

To link to this article: https://doi.org/10.1080/17686733.2018.1557453

Published online: 19 Mar 2019.

QUANTITATIVE INFRARED THERMOGRAPHY JOURNAL
2019, VOL. 16, NO. 1, 129–145
https://doi.org/10.1080/17686733.2018.1557453

Taylor & Francis
Taylor & Francis Group

RESEARCH ARTICLE

Method of classification of global machine conditions based on spectral features of infrared images and classifiers fusion

Marek Fidali and Wojciech Jamrozik

Faculty of Mechanical Engineering, Silesian University of Technology, Institute of Fundamentals of Machinery Design, Gliwice, Poland

ABSTRACT

This paper describes an original method of global machine condition assessment for infrared condition monitoring and diagnostics systems. This method integrates two approaches: the first is processing and analysis of infrared images in the frequency domain by the use of 2D Fourier transform and a set of F-image features, the second uses fusion of classification results obtained independently for F-image features. To find the best condition assessment solution, the two different types of classifiers, *k*-nearest neighbours and support vector machine, as well as data fusion method based on Dezert–Smarandache theory have been investigated. This method has been verified using infrared images recorded during experiments performed on the laboratory model of rotating machinery. The results obtained during the research confirm that the method could be successfully used for the identification of operational conditions that are difficult to be recognised.

ARTICLE HISTORY
Received 10 April 2018
Accepted 6 December 2018

KEYWORDS
Classification; decision fusion; PCR6; infrared image analysis; Fourier analysis; infrared thermography; condition base monitoring

1. Introduction

Infrared thermography is a modern and popular technique for thermal condition monitoring of machinery, apparatus and industrial processes [1].

Infrared cameras can be used in continuous condition monitoring systems for contactless detection and identification of object faults at its early stage, which is useful for planing object maintenance and overhauls.

A continuous condition monitoring system based on the infrared device should include infrared image processing and recognition to classify the current operating condition of the object. Research connected with the application and development of infrared image processing and analysis, as well as artificial intelligence methods, to continuous thermographic objects monitoring and diagnostics has been carried out in several different academic and research centres [2,3] and also by the authors [4]. In this article, an original method of object condition identification, which can be used in continuous condition monitoring and diagnostics systems, has been proposed.

The method can be generalised to any diagnostic data acquired during continuous monitoring of different objects or industrial processes.

CONTACT Marek Fidali marek.fidali@polsl.pl Silesian University of Technology, Institute of Fundamentals of Machinery Design, Kochanowskiego 18a, Gliwice 44-100, Poland

2. Method

It has been assumed that the assessment of the general condition of an object could be determined on the basis of the analysis of infrared images that are acquired continuously by monitoring the system during an object operation.

For a clear description of the method, let us assume that the diagnosed object is a complex machinery containing several sub-assemblies (e.g. motor, couplings, journal bearing, pomp, etc.).

Having acquired an infrared image of machinery at any moment of its operation, it is possible to define regions of interests (ROIs) containing only important parts of the diagnosed object. In such a way, the rest of the image content could be treated as an unwanted background that is not considered during the diagnostic process.

In the proposed method, whose brief algorithm is presented in Figure 1, each defined ROI contained a sub-assembly of the machinery that could be treated as a kind of sub-image. Each sub-assembly in a different way reflects the machine's conditions; thus, the analysis of the sub-images of sub-assemblies allows us to acquire partial diagnostic information about global conditions of an object. The process of analysis of each sub-image gives sets of features that represent the condition of each machine sub-assembly at the moment of its operation corresponding to the time of infrared image acquisition. The local conditions of the sub-assemblies are related to the machine's global condition.

Having determined the feature vectors for infrared images acquired during machine operation in different conditions (including faults), it is possible to design a set of local classifiers that allow us to identify conditions of the machinery. At this stage, the classifiers could be treated as local experts.

Local diagnostic information provided by each classifier can be joined together to get information about global (overall) machinery condition. In the elaborated method, to aggregate diagnostic decisions and maximise final classification performance, application of decision fusion methods was used.

2.1. Processing and analysis of infrared images

The versatile nature of the developed method allows us to apply different image processing and analysis methods to obtain a features set. For method verification purposes, the authors decided to use the spectral representation of infrared images. The spectral representation of infrared images is obtained by use of the two-dimensional (2D) Fourier transform. One of the reasons for application of the 2D Fourier transform is a shift-invariant property [5], which makes the method less sensitive to deviation in the location of imagining device while observing an object. The spectral representation of infrared image could also emphasise diagnostic information that could be hidden in the real image.

The result of Fourier transform of an infrared image is a 2D spectrum, which could be represented by two images of magnitude and phase called also F-images. Frequency components on the F-images are distributed symmetrically, and in many cases of the analysis, it is enough to consider one-quarter of the magnitude (grams) and/or two adjacent quarters of the phase (grams). In most considered cases, the entire F-image is shown and analysed [4,5]. This approach is most convenient for F-image interpretation purposes because frequency components generate specific symmetrically distributed

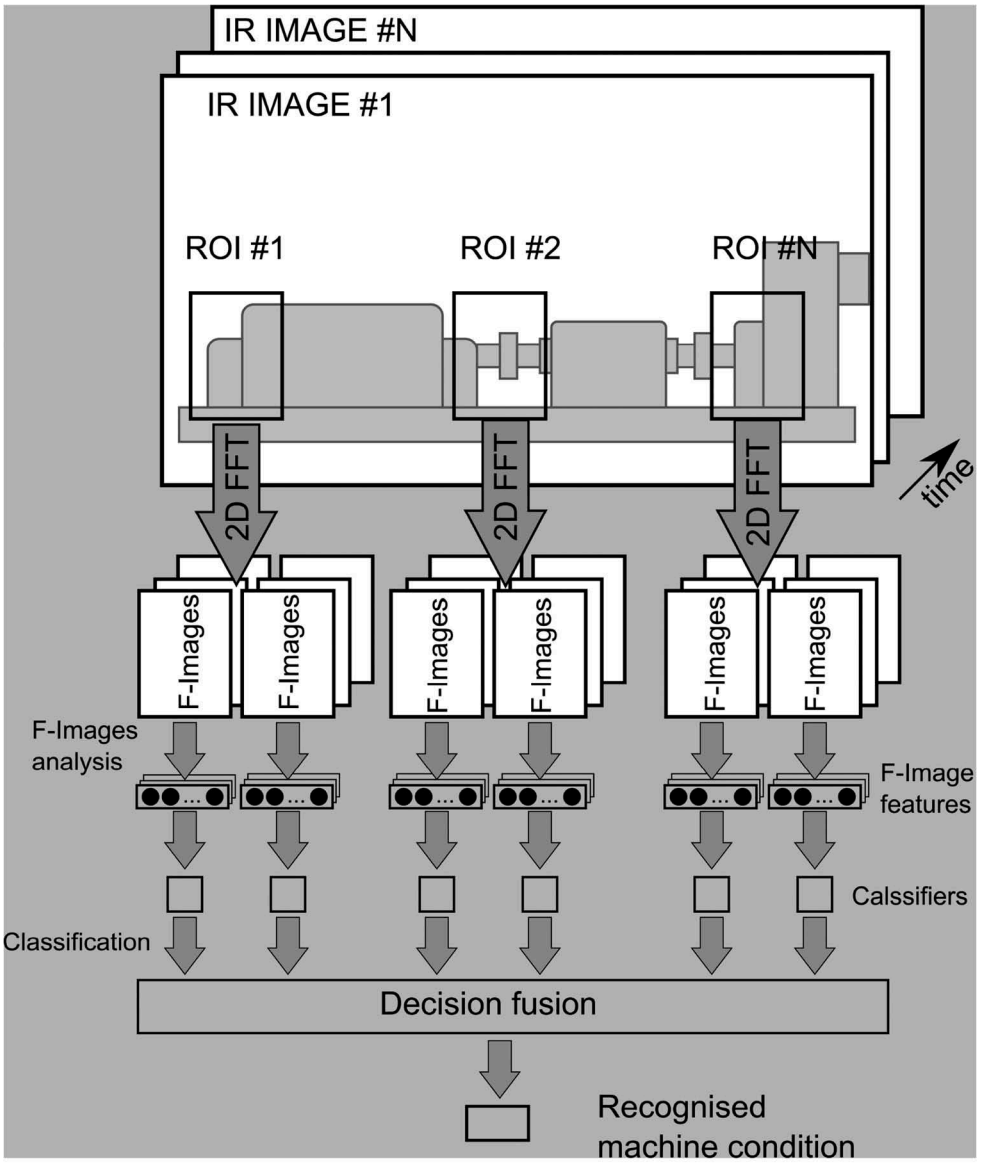

Figure 1. Idea of the method of identification of object conditions based on infrared images.

patterns (similar to stars) (c.f. Figure 2), whose shapes and locations depend on a content of the original infrared image.

To analyse the F-images, the three following features are defined:

HFP – Horizontal F-image Parameter,
VFP – Vertical F-image Parameter,
CFP – Circular F-image Parameter.

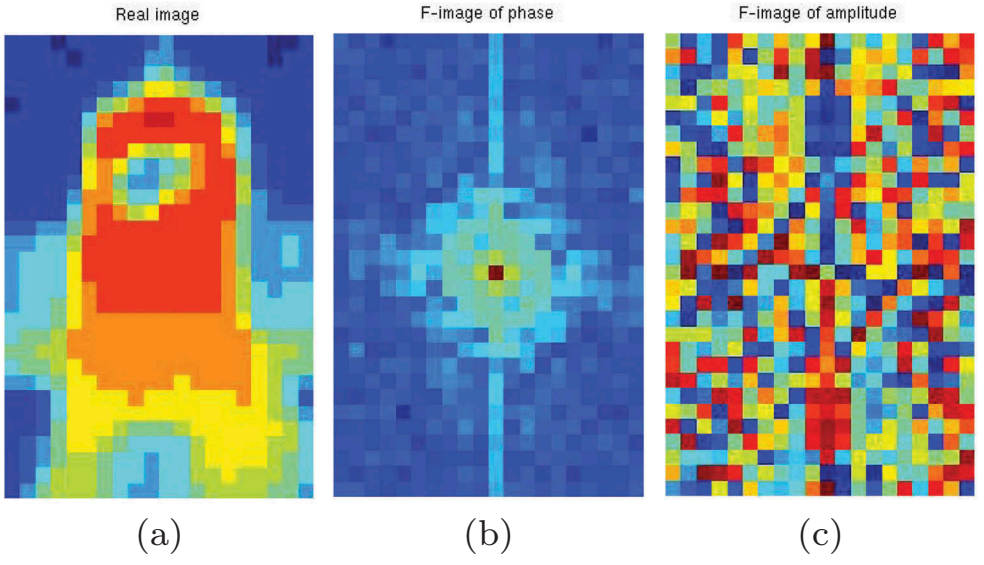

Figure 2. An exemplary infrared image (a) and its F-images of magnitude (b) and phase (c) obtained on the basis of 2D Fourier analysis.

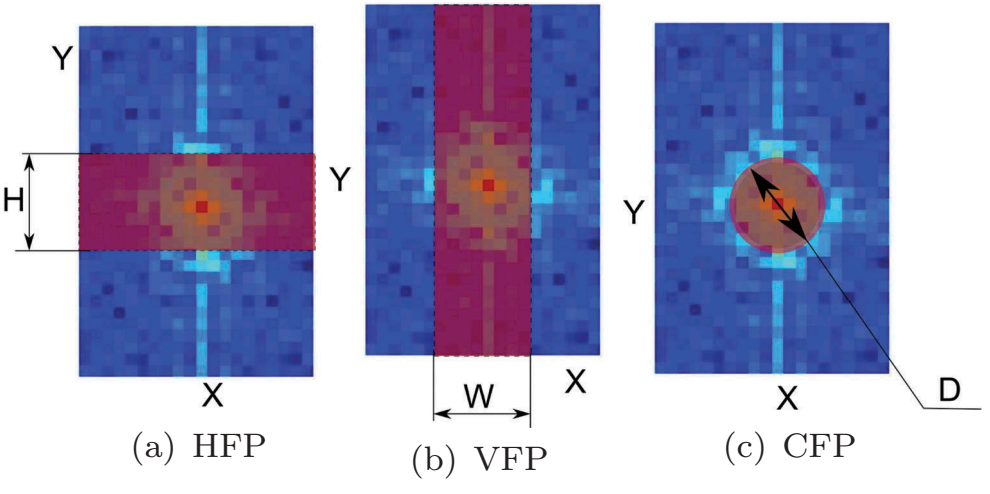

Figure 3. Graphical illustration of considered features of F-images.

The features are mean values of F-images frequency components calculated over rectangular and circular areas, placed in the centres of the F-images in the way presented in Figure 3. The dimensions of areas that were used to calculate the feature values were set experimentally (c.f. 3.1)

2.2. Classification of the machine's conditions

To classify machine operating conditions, a number of possible approaches could be chosen [6]. In practice, the choice of a classifier is a difficult problem and it is often based on a data

specificity, as well as a researcher's experience. The authors decided to apply two classifiers: a simple *k*-nearest neighbour (k-NN) classifier [7] and support vector machine (SVM) [8], which is recognised as a very effective classification solution. The author's intention was to show how to use the method and how the different classifiers behave.

To obtain a reliable and certain classification efficiency, the *leave-one-out* cross-validation (LOOCV) algorithm [9] has been applied.

The LOOCV validation method has a high variance, but estimates of generalization error are comparable with other partitioning schemes used for classification efficiency evaluation [10].

The classifier accuracy measure that we used was the relative number of misclassification, which is calculated as follows: $err = N_e/N$

where N is the number of considered samples and N_e is the number of misclassified samples. On the basis of the *err* measure, the classifier efficiency was calculated in the following way: $eff = (1 - err) \cdot 100\%$.

2.3. Decision fusion

In the elaborated method, joining of the classification results is proposed. There are some methods which allow treatment of the data jointly [11]. One of the interesting approaches is a decision fusion.

Decision fusion, which is also called classifier fusion, is the method that combines the results of classification obtained from different classifiers trained over different types of data gathered from the same object. In this approach, classifiers are treated as 'local experts', who make decision about the machine's condition.

The use of classifiers in technical diagnostic is connected with the uncertainty of the data on which those classifiers are trained. The sources of uncertainty could take the following form, for example, [12]: random events, measurement deviations, incompleteness of the set of considered diagnostic parameters and lack of knowledge about diagnosed object or process.

In general, most types of uncertainty could be characterised by the use of classical probability theory based on the Bayesian theorem [13,14].

An alternative to the Bayesian methods is the Dempster–Shafer Theory (DST), also called the mathematical theory of evidence. The DST can deal with imprecise or incomplete data. In addition, DST can be interpreted as a generalisation of probability theory where probabilities are assigned to multiple possible events (e.g. sets of events) as opposed to mutually exclusive singletons [15,16].

The DST offers very important mechanisms of information aggregation coming from multiple sources by the use of rules for combining evidences. A lot of rules have been developed since establishing the DST.

Several interesting examples, including a detailed analysis of validity of Dempster's combination rule in different contexts, can be found in [17–19].

A generalisation and in some points an extension of the DST is The Dezert–Smarandache Theory (DSmT) [20] of plausible and paradoxical reasoning. DSmT overcomes some limitations of DST [20,21] because it allows us to formally combine any kind of information. DSmT bases itself on similar terms as DST. The DSmT introduces the generalised frame of discernment Θ, which contains n exhaustive elements $(\theta_1, \ldots, \theta_n)$. In the classification case, elements of Θ are all considered classes (class labels).

On the basis of the generalised frame of discernment, hyper-power set D^{Θ} can be created of all single class labels but also of allowed class labels logical combinations. This means that classification can not only be made for single classes but the tested sample can also be assigned simultaneously to several classes ($\theta_i \cap^{\theta_k} \neq \emptyset$) or there can be some uncertainty in the reasoning process and the same test sample can be member of one or other class ($\theta_i \cup^{\theta_k} \neq \emptyset$). Each of these combinations is called focal element. For each element of D^{Θ}, a Generalised Basic Belief Assignment (GBBA) is possible. In other words, as the result of classification, some belief is assigned for test sample x that is a member of certain classes, several classes or there is some doubt to which class it should be assigned. From the formal site: $m(.) : D^{\Theta} \rightarrow [0, 1]$ so GBBA can take values from 0 to 1, and if $m_x(A) = 1$, there is 100% belief that test element x belongs to class A. In contrast, for an empty set – e.g., unknown class $m(\emptyset) = 0$. Belief assigned to all elements of D^{Θ} should sum up to 1: $\sum_{A \in D^{\Theta}} m(A) = 1$. This means that in the frame of discernment, D^{Θ} tested elements are for sure member of one of classes or class combinations defined by D^{Θ}; so, no other unknown classes are allowed.

Similar to DST, the DSmT also allows to aggregate information with the use of combination rules. For this purpose, many combination rules have been elaborated [20,22]. During the research, a PCR6 rule was used. The key idea of the PCR6 rule is to transfer the partial conflicting Basic Belief Assignment (BBA) proportionally to the individual BBA of non-empty elements involved in the conflict [23].

2.4. GBBA calculation

The calculation of evidence is crucial for classifier fusion based on the methods demanding the BBA or the GBBA for each class [24,25].

A simple method, which is ideal for research at the preliminary stage, has been developed for the evidence calculation from k-NN classifiers [26]. To obtain the output for a given sample, a set of distance measures to a number of known samples is calculated and it can be regarded as a class distribution. Identification of k -NNs of a element x irrespective of the class label is made. Then, the number of neighbours k_i supporting assignment of an element x to class C_i is calculated. Accordingly, the *GBBA* function of class C_i is calculated as follows [26]: $m(\{C_i\}) = k_i/k$

In case of SVM classifier, which unfortunately gives only class labels, the probabilities of class distribution were obtained applying extension introduced by Wu [27]. In the presented research, we deal with only one occurring condition at the time; therefore, probabilities are very useful. It can be assumed that SVM classifier outputs are degrees of support for each class representing identified machine conditions. These outputs can be directly transformed into mass assignments: $p_i \rightarrow m(i)$, where p_i is the probability of condition i occurrence and $m(i)$ is the belief that condition i occurred provided by single SVM classifier on the basis of available evidence (in a form of feature space).

3. Method verification

Our method verification considers several different aspects of the method's application. First of all, verification should confirm that the method can be useful in condition monitoring of

machinery. The second important task of verification was to indicate what kind of classifier should be used and what is the best way to perform data fusion. To do this, we use two earlier described classifiers and compare results of classification obtained by use of single classifiers with results of classifier fusion, as well as results of classification obtained for multidimensional space of features. Investigation helps us to find the best solution to answer the question: is fusion of simple classifiers a better solution than the application of the classifier to single or multidimensional space of features? The method was verified on the basis of digital infrared images taken during diagnostic experiments. All of our computations were performed using Matlab 2007b software.

3.1. Considered experimental data

The experiments have been performed using a laboratory stand that consists of a laboratory model of rotating machinery and an infrared imagining system (Figure 4).

During the experiment, a sequence of 840 infrared images of resolution 320 × 480 pixels has been recorded. The thermographic images have been taken every 30 s. The images have represented the machine operating in the conditions presented in Table 1.

For reference, condition S1 decided to record two times more images to make it easier to recognise by classifiers. It should be pointed out that conditions S2, S3 and S4 are difficult to distinguish and have been simulated intentionally to check whether it was possible to notice a small change in operational condition. Such small changes were also desirable for testing the ability of the classifiers to recognise nearly indistinguishable changes in the machine's condition.

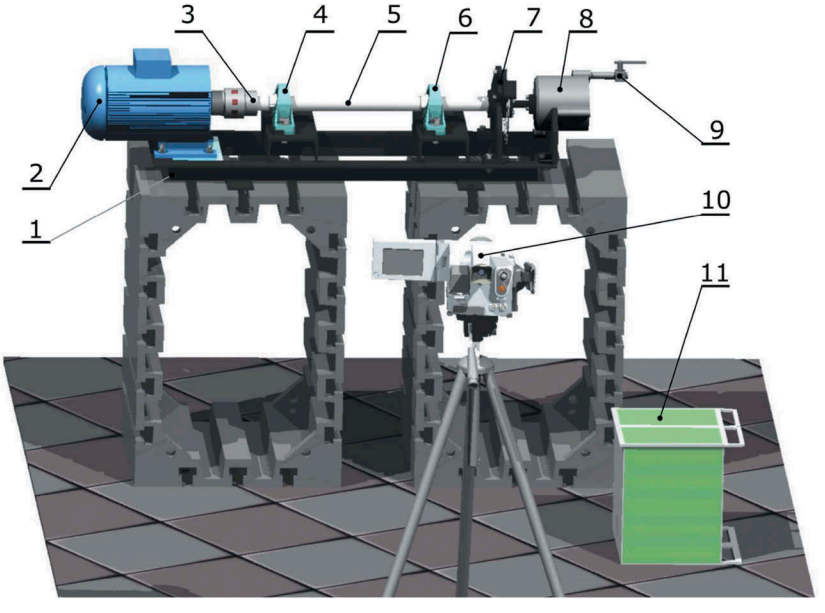

Figure 4. Visualisation of the laboratory stand. 1-frame, 2-motor (1.5 kW, 2500 rpm), 3-coupling, 4-bearings set no 1, 5-shaft, 6-bearings set no 2, 7-break set, 8-air pump, 9-throttle valve, 10-infrared camera connected to PC, 11-motor controller.

Table 1. Description of conditions simulated during the experiment.

Condition Id	Description of fault	No. of acquired images
S1	Machine without faults	240
S2	50% Throttling of air pump	120
S3	90% Throttling of air pump	120
S4	90% Throttling of air pump and clearance of second bearing mounting	120
S5	Load of disk brake	120
S6	Faulty bearing no. 2	120

The infrared images acquired during the experiment have been preprocessed. The first step of the preprocessing was the selection of two ROIs of size 20 × 30 pixels (ROI1 and ROI2) (Figure 5). These ROIs represented the bearing housings. It was expected that changes in the machine's condition would affect changes in bearing temperature and should be revealed in the infrared images.

According to the proposed method (c.f. 2), sub-images corresponding to ROI(ROI1 and ROI2) were transformed to the frequency domain using Fast Fourier Transform algorithm. F-images (magnitude and phase) obtained after transformation were analysed, and image features were calculated. Each infrared image was represented by 12 features, whose names were coded in the following way:

EstimatorId_FImageType_ROIId

e.g. HFP_P_R1 means that the value of the feature HFP was calculated for F-image of phase determined in ROI1.

It is obvious that the values of presented F-image features depend on dimensions and content of the ROI, as well as type of F-image (magnitude and phase). To consider a variety in the content of each type of F-images, each of the proposed features could be fitted to the image content by setting a value of the feature parameter W, H and D.

To find the optimal values of F-image feature parameters W, H and D, an exhaustive search of feature space based on criterion of the maximum machine conditions classifier performance has been performed. Features have been calculated for each acceptable value of the feature parameters (from 1 to the maximal value $H_{max} = 30, W_{max} = 20, D_{max} = 20$).

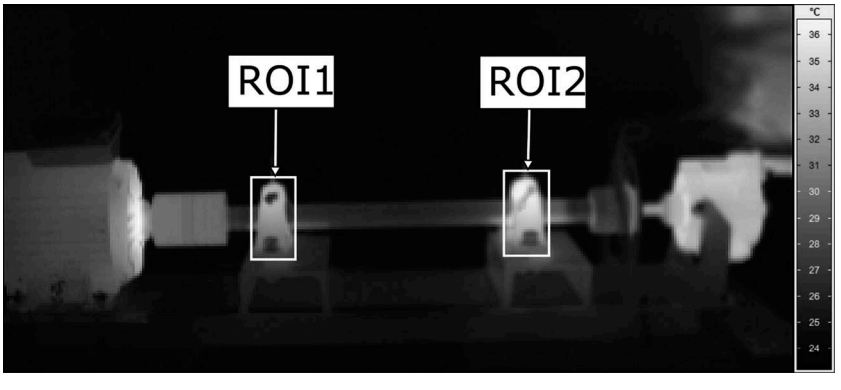

Figure 5. Infrared image of the operating laboratory stand, with marked ROIs of the first (left, ROI1) and the second (right, ROI2) bearings.

Table 2. Optimal values of feature parameters and basic statistics of classification efficiencies.

Feat. Num.	Feat. Name	Estimator Parameter Name	Estimator Parameter Value	Mean Eff. [%]
1	ROI1_VFP_A	H	20	59.6
2	ROI2_VFP_A	H	18	80.6
3	ROI1_VFP_P	H	2	23.9
4	ROI2_VFP_P	H	7	25.2
5	ROI1_HFP_A	W	29	56.9
6	ROI2_HFP_A	W	26	80.8
7	ROI1_HFP_P	W	9	28.3
8	ROI2_HFP_P	W	9	24.3
9	ROI1_CFP_A	D	14	62.3
10	ROI2_CFP_A	D	20	75.6
11	ROI1_CFP_P	D	6	37.1
12	ROI2_CFP_P	D	6	43.4

Constrains followed from the size (20×30 pixels) of the considered F-images. For optimisation purposes, a *k*-NN classifier was used. A number of nearest neighbours parameter was set to $k = 10$ according to recommendations presented in [28]. Classification efficiency was calculated in the way presented in the theoretical background (c.f. 2.2) and LOOCV algorithm was used. Optimal values of feature parameters are presented in Table 2.

The feature values, calculated using determined optimal parameters of F-image features, were the data source for classification of machine conditions.

3.2. Classification results for one- and multidimensional feature space

The first step of the method verification was assessment of the application of one- (1D) and multidimensional F-images feature space for purposes of classification of machine condition. As mentioned earlier, *k*-NN and SVM classifiers were applied. In case of *k*-NN classifier, a $k = 10$ neighbours was used. The Euclidean distance function was used as a distance metric in *k*-NN classifier. In case of SVM classifier, one-against-all strategy is implemented for multi-class classification. A Gaussian kernel was applied. Mean classifier efficiencies of considered machine conditions as a function of feature space dimension were shown in Figure 6. As one can expect, classification efficiency increase with size of feature space and for almost all conditions reach efficiency above 80% for size of feature space equal to 4 and more. A detailed analysis of maximal classifier efficiencies is presented in Table 3. The results show that in case of conditions S1, S3, S4, S5 and S6, maximum efficiencies could be achieved for 1D space of feature values for both types of applied classifiers. Values of maximal classification efficiencies are given in bold. The highest classification efficiency values have been obtained on the basis of CFP feature, which indicates its usefulness in analysing the F-images. The greatest number of maximum classification efficiency (100%) was obtained using the SVM classifier. SVM gave the best results for features of F-images of phase, whereas *k*-NN gave good results for F-images of magnitude within the ROI2. Region ROI2 covered more load bearing support, which affected its highest temperature and thus intensive infrared radiation.

A plot of classification efficiencies for condition S2 presented in Figure 6 and values in Table 3 clearly show that condition S2 is poorly recognisable. Analysis of classification

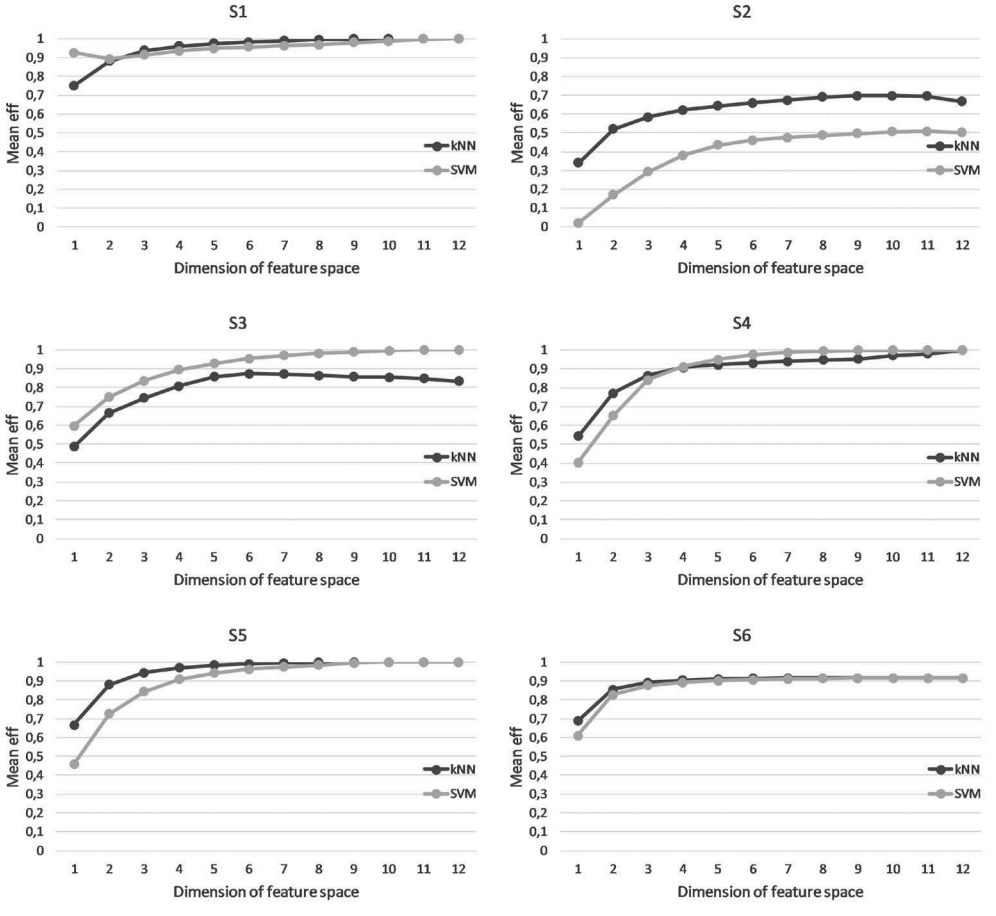

Figure 6. Plots of mean classifiers efficiencies as a function of feature space dimension for considered conditions.

efficiencies for condition S2 shows that application of 1D feature space allowed to obtain maximal efficiency equals 58.3% with application of *k*-NN classifier. The SVM classifier was unable to correctly recognise condition S2, where SVM allowed to obtain maximal efficiency of 8.3%.

Looking at feature values distribution for condition S2 presented in Figure 7, it is clear that SVM was unable to find proper global decision boundaries. Exemplary decision boundary for condition S2 vs. all other conditions can be seen in Figure 7. Taking into consideration the distribution of feature values for condition S2, the strategy of classification using SVM classifier with linear boundaries is insufficient to distinguish between S2 and other classes. Application of feature spaces dimensionality of 3–8 increases maximal classification performance of condition S2 which was, respectively, 83% for *k*-NN and 75% for SVM classifiers. Minimal space giving maximal classification performance with the use of *k*-NN classifier was constructed with the use of the following two sets of features:

Table 3. Classification efficiencies obtained for individual F-image features.

	Simulated machine conditions					
Feature space	S1	S2	S3	S4	S5	S6
kNN(HFP_A_R1)	62.5	16.7	91.7	33.3	91.7	91.7
SVM(HFP_A_R1)	87.5	0.0	**100.0**	0.0	83.3	91.7
kNN(HFP_P_R1)	54.2	16.7	8.3	25.0	25.0	16.7
SVM(HFP_P_R1)	87.5	0.0	**100.0**	0.0	83.3	91.7
kNN(HFP_A_R2)	91.7	58.3	41.7	83.3	**100.0**	91.7
SVM(HFP_A_R2)	83.3	8.3	**100.0**	83.3	**100.0**	83.3
kNN(HFP_P_R2)	50.0	16.7	8.3	8.3	16.7	8.3
SVM(HFP_P_R2)	**100.0**	0.0	0.0	0.0	0.0	0.0
kNN(VFP_A_R1)	58.3	8.3	**100.0**	58.3	91.7	91.7
SVM(VFP_A_R1)	79.2	0.0	**100.0**	16.7	75.0	91.7
kNN(VFP_P_R1)	50.0	0.0	0.0	8.3	16.7	16.7
SVM(VFP_P_R1)	**100.0**	0.0	0.0	0.0	0.0	0.0
kNN(VFP_A_R2)	91.7	58.3	25.0	83.3	**100.0**	91.7
SVM(VFP_A_R2)	83.3	8.3	**100.0**	83.3	**100.0**	83.3
kNN(VFP_P_R2)	62.5	0.0	16.7	25.0	8.3	16.7
SVM(VFP_P_R2)	95.8	0.0	0.0	0.0	25.0	16.7
kNN(CFP_A_R1)	87.5	16.7	91.7	0.0	91.7	83.3
SVM(CFP_A_R1)	**100.0**	8.3	**100.0**	25.0	75.0	83.3
kNN(CFP_P_R1)	62.5	0.0	0.0	8.3	25.0	16.7
SVM(CFP_P_R1)	**100.0**	0.0	**100.0**	75.0	0.0	**100.0**
kNN(CFP_A_R2)	91.7	58.3	75.0	91.7	**100.0**	91.7
SVM(CFP_A_R2)	83.3	0.0	**100.0**	91.7	91.7	83.3
kNN(CFP_P_R2)	62.5	50.0	16.7	33.3	8.3	41.7
SVM(CFP_P_R2)	**100.0**	0.0	16.7	**100.0**	0.0	58.3

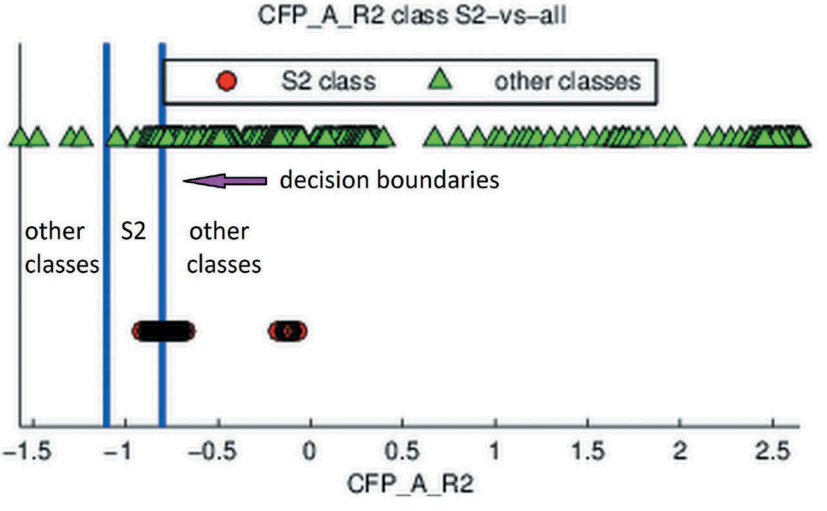

Figure 7. Distribution of CFP_A_R2 feature for condition S2.

VFP_P_R2, *HFP_A_R2*, *HFP_P_R2* and

VFP_A_R1, *HFP_P_R2*, *CFP_A_R1*

To assess which classes are most similar, a confusion matrix was prepared (Figure 8). In each column, there is percentage fraction of each class that was assigned to various

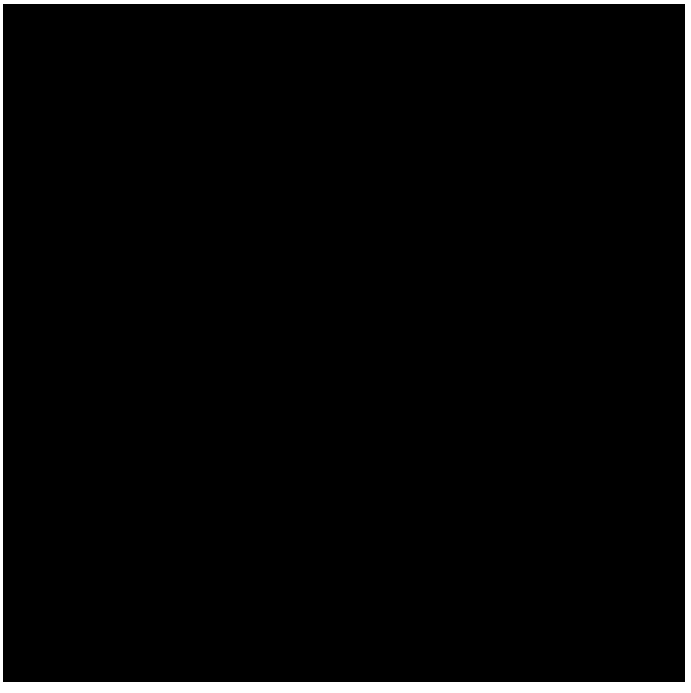

Figure 8. Normalised confusion matrix for single *k*-NN classifier.

predicted classes. Taking into consideration only single *k*-NN classifiers, that were trained over 1D data set it can be seen, that conditions S2 and S3 are most difficult to distinguish. It is connected with the way in which those conditions were simulated, when only degree throttling of air pump was changed.

4. Classifier fusion results

Results of the classification of machine conditions, shown in Section 2.2 (Table 3), indicate that the proposed features of the F-images are useful for assessing machine conditions. For the majority of concerned machine conditions, it was possible to obtain the maximum classification efficiency on the basis of selected individual features of F-images. However, for condition S2, reliable condition assessment was not possible. To increase classification efficiency, fusion of classifiers was applied. We carried out an exhaustive computation considered all combinations of two, three and four *k*-NN and SVM classifiers of all considered F-image features. Mean classification efficiencies after classifier fusion as a function of number of fused classifier for all considered conditions are presented in Figure 9. Table 4 presents the highest classification efficiencies obtained for all condition after fusion of two, three and four combinations of different individual *k*-NN and SVM classifiers. Our results show that fusion of two classifiers is sufficient to obtain maximal classification almost for all conditions. Classifier fusion also allowed us to raise the highest classification efficiency for condition S2 by 8.3% (from 58.3% to 66.7%) in comparison to the results obtained for the individual classifiers. The maximum efficiency of the classification was obtained as a result of the fusion of *k*-NN

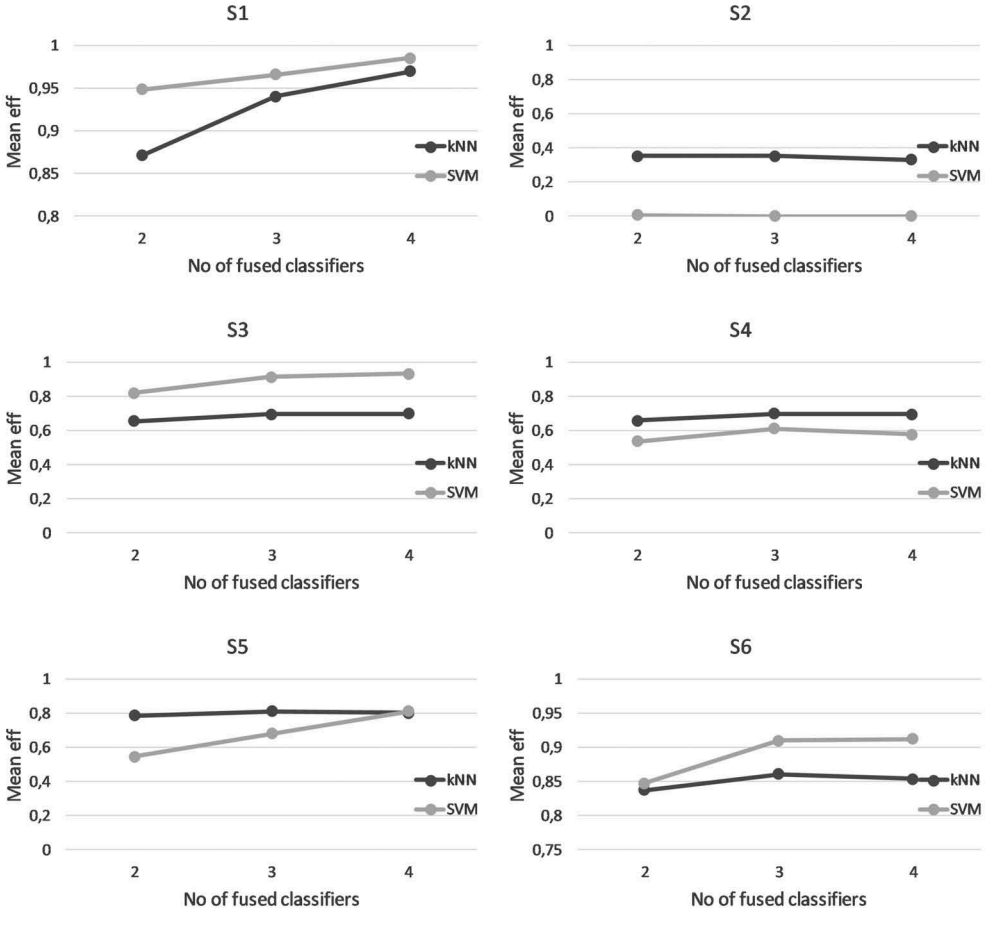

Figure 9. Plots of mean classification efficiencies as a function of different number of fused classifiers for considered machine conditions.

Table 4. Comparison of maximal classification efficiencies for all conditions after fusion different numbers of single *k*-NN and SVM classifiers using PCR6 rule.

		Simulated machine conditions					
Fuzz. Class. No.	Class. Type	S1	S2	S3	S4	S5	S6
2	kNN(.)	100.0	66.7	100.0	100.0	100.0	100.0
	SVM(.)	100.0	8.3	100.0	100.0	100.0	100.0
3	kNN(.)	100.0	66.7	100.0	100.0	100.0	100.0
	SVM(.)	100.0	8.3	100.0	100.0	100.0	100.0
4	kNN(.)	100.0	66.7	100.0	100.0	100.0	100.0
	SVM(.)	100.0	8.3	100.0	100.0	100.0	100.0

classifiers only. Fusion of the SVM classifiers does not ensure an increase of the classification efficiency for this class.

The most interesting observation made after the analysis of classification performances is the lack of an increase of the efficiency for the condition S2 according to the number of fused single classifiers. This is caused by the presence of the classifiers that assign the high

Table 5. Comparison of maximal classification efficiencies for all conditions fusion of two classifiers trained over 2D feature space.

		Simulated machine conditions					
Fuzz. Class. No.	Class. Type	S1	S2	S3	S4	S5	S6
2	kNN(.)	100.0	83.3	100.0	100.0	100.0	100.0
	SVM(.)	100.0	62.5	100.0	100.0	100.0	100.0

degree of belief to the wrong states. Fusing more than two classifiers did not cause an increase of the relative number of classifier combinations giving the maximal performance. These results find confirmation in [29], which showed that adding additional experts at some point leads to obtaining totally conflicted and useless classifier combinations. Analysis of classifiers combinations giving the highest performances indicates that they are composed of complementary rather than individually best-performing classifiers. Taking into account the obtained results, it can be concluded that the fusion of two selected classifiers is sufficient. In case of the considered data, a pair of classifiers assuring highest efficiency 66.7% was HFP_A_R2, CFP_A_R1.

Taking into consideration the very good results of classification obtained for multidimensional feature spaces decided to perform fusion of *k*-NN classifiers calculated for two-dimensional feature spaces. As could have been expected, the results were very good (Table 5). Maximal classification efficiency for condition S2 was increased to 83.3% for four following combination of classifiers and feature spaces:

PCR6{kNN{VFP_A_R2,CFP_A_R2},kNN{HFP_P_R2,CFP_A_R1}},
PCR6{kNN{HFP_P_R2,CFP_A_R1},kNN{HFP_P_R2,CFP_A_R2}},
PCR6{kNN{HFP_P_R2,CFP_A_R1},kNN{HFP_P_R2,CFP_P_R2}},
PCR6{kNN{HFP_P_R1,CFP_P_R1},kNN{HFP_P_R2,CFP_A_R1}}.

Its worth mentioning that maximal classification efficiency using single *k*-NN classifier for condition S2 with the use of three- and four-dimensional (3D and 4D) space of feature was also 83.3%. The presented results confirm the ability of decision fusion algorithms to identify machinery conditions which are difficult to be recognised. In contrast, the SVM classifier results for the 2D feature space was maximally 62.5%. Accordingly, the increase of classification performance in comparison to single feature space is visible, and in this the *k*-NN classifier was proven to be better than the SVM classifier.

5. Conclusions

In this paper, the method of object condition assessment using multiple classifiers fusion approach based on the generalised evidence theory is proposed. Fused classifiers have been trained over the data represented by three parametric spectral features of F-images. The F-images were the result of the 2D Fourier transform of infrared images acquired during object observation. During the research, optimal parameters of the features were evaluated and F-image features were computed. Based on the spectral features of the infrared images the classification process was performed. For comparison purposes, *k*-NN and SVM classifiers were used. The results of the classification have

shown that the proposed features of an F-image of thermograms could be useful for the evaluation of a machine's condition. Circular F-image Parameter (CFP) seemed to be suitable enough for the estimation of magnitude, as well as phase F-images.

The proposed approach of classifier fusion is suitable for the assessment of machine global condition on the basis of preselected features of spectral infrared images. Classification efficiencies obtained using classifier fusion are higher than those calculated taking into consideration a single classifier. It must be mentioned that features chosen for the member classifiers in fusion process should be heterogeneous to assure high classification efficiency. Moreover, the increase of the number of considered ROIs should entail a reduction of the uncertainty of the information, which is used in the decision-making about the machine's global condition. Although the connection between the diversity of features and the classification performance is not always straightforward, the analysis of the obtained results leads to the statement that in the considered case, the influence of feature heterogeneity degree on the fusion results is quite noticeable. The problem of high homogeneity of data could be resolved by classification of multidimensional space of homogeneous feature values and the next application of the fusion of such a classifier. This strategy was verified during the presented research and the obtained results confirmed the ability of classifier fusion to increase classification efficiency of condition S2, which was difficult to recognise.

It can be expected that conclusions made from the research could be generalised to data represented by other infrared image features and diagnostic signals. However, it needs further investigation.

Disclosure statement

No potential conflict of interest was reported by the authors.

Notes on contributors

Marek Fidali is an associate professor in the Institute of Fundamentals of Machinery Design at the Faculty of Mechanical Engineering of the Silesian University of Technology since 2015. He received the Master of Science and PhD degrees in Mechanical Engineering from Silesian University of Technology in 1997 and 2003, respectively. His research interests lie in technical diagnostics in the broad sense, infrared thermography, images and signals processing methods as well as modal analysis, measurement systems and acoustics.

Wojciech Jamrozik Assistant professor in the Institute of Fundamentals of Machinery Design at the Faculty of Mechanical Engineering of the Silesian University of Technology. He received the PhD degree in Mechanical Engineering from Silesian University of Technology in 2012. His main research areas are technical diagnostics, image processing, and analysis, as well as aggregation of incomplete and uncertain information in technical diagnostics.

References

[1] Thomas RA. The thermography monitoring handbook. Oxford, UK: Coxmoor Pub.; 1999. (Machine & systems condition monitoring series).

[2] Younus AM, Yang BS. Intelligent fault diagnosis of rotating machinery using infrared thermal image. Expert Syst Appl. 2012;39:2082–2091.

[3] Widodo A, Satrijo D, Prahasto T, et al. Confirmation of thermal images and vibration signals for intelligent machine fault diagnostics. Int J Rotating Mach. 2012;2012:1–10.
[4] Fidali M. Methodology of thermographical diagnostics of technical object (in polish). Gliwice: Wydawnictwo Naukowe Instytutu Technologi Eksploatacji - PIB; 2013.
[5] Nixon SM, Aguado S. Feature extraction and image processing. Oxford, Boston: Newnes; 2002.
[6] Jain AK, Duin RP, Mao J. Statistical pattern recognition: a review. IEEE Trans Pattern Anal Mach Intell. 2000;22(1):4–37.
[7] Cunningham P, Delany SJ. k-nearest neighbour classfiers. Technical report UCD-CSI-2007-4; 2007.
[8] Vapnik VN. The nature of statistical learning theory. Berlin, Heidelberg: Springer-Verlag; 1995.
[9] Evgeniou T, Pontil E. M, Elisseeff A, Leave-one-out error, stability, and generalization of voting combinations of classifiers, Mach. Learning. 2004;55(1):71–97.
[10] Kohavi R. A study of cross-validation and bootstrap for accuracy estimation and model selection. In: IJCAI'95 Proceedings of the 14th international joint conference on Artificial intelligence. Montreal: Morgan Kaufmann; 1995. 1137–1145.
[11] Fidali M. Method of machine technical state assessment on the basis of joint signal analysis. Mech Syst Signal Process. 2011;25(3):871–883.
[12] Korbicz J, Kościelny J, Kowalczuk Z, et al. editors. Fault diagnosis. Models, artificial intelligence, applications. Berlin: Springer; 2004.
[13] Bednarski M, Cholewa W, Frid W. Identification of sensitivities in bayesian networks. Eng Appl Artif Intell. 2004;17(4): 327–335. Selected problems of knowledge representation.
[14] Subrahmanya N, Shin YC, Meckl PH. A bayesian machine learning method for sensor selection and fusion with application to on-board fault diagnostics. Mech Syst Signal Process. 2010;24(1):182–192.
[15] Shafer G. A mathematical theory of evidence. Mercer County, NJ: Princeton University Press; 1976.
[16] Dempster A. Upper and lower probabilities induced by a multivalued mapping. Ann Math Statist. 1967;38:325–339.
[17] Wang P. A defect in Dempster-Shafer theory. In: Ramon Lopez de Mantaras, David Poole, editors.Proceedings of the tenth conference on uncertainty in artificial intelligence. Morgan Kaufmann Publishers; 1994. p. 560–566.
[18] Dezert J, Wang P, Tchamova A. On the validity of Dempster-Shafer theory. In: 15th international conference on information fusion (FUSION'12), July, 2012, Singapore, p. 655–660.
[19] Smarandache F, Dezert J. Modified pcr rules of combination with degrees of intersections. In: 18th international conference on information fusion, July, Washington, DC, USA, 2015, p. 2100–2107.
[20] Dezert J, Smarandache F, DSmT: A New Paradigm Shift for Information Fusion. In: Proceedings of Cogis ' 06 Conference, Paris, March 2006, pp. 15–17
[21] Zadeh L. On the validity of dempster's rule of combination. Berkely: University of California; 1979. (UCB/ERL M79/24).
[22] Smets P, Kennes R. The transferable belief model. Artif Intell. 1994;66:191–234.
[23] Smarandache F, Dezert J. On the consistency of pcr6 with the averaging rule and its application to probability estimation. In: Proceedings of the 16th international conference on information fusion, July, Istanbul, Turkey, 2013, p. 1119–1126.
[24] Xu L, Krzyzak A, Suen C. Methods of combining multiple classifiers and their applications to handwriting recognition. Syst Man Cybernet IEEE Trans. 1992;22(3):418–435.
[25] Zhang B, Srihari S. Class-wise multi-classifier combination based on Dempster-Shafer theory. In: 7th international conference on control, automation, robotics and vision (ICARCV), Vol. 2, December, Marina Mandarin, Singapore, 2002, p. 698–703.
[26] Han D, Han C, Yang Y. Multiple k-nn classifiers fusion based on evidence theory. In: IEEE international conference on automation and logistics, August, Jinan, China, 2007, p. 2155–2159.

[27] Wu TF, Lin CJ, Weng RC. Probability estimates for multi-class classi cation by pairwise coupling. J Mach Learn Res. 2004;5:975–1005.
[28] Batista GEAPA, Monard MC. A study of k-nearest neighbour as an imputation method. In: Second international conference on hybrid intelligent systems, December, Maebashi City, Japan, 2002, p. 251–260.
[29] Martin A, Jousselme AL, Osswald C. Conflict measure for the discounting operation on belief functions. In: 11th international conference on information fusion, July, Cologne, Germany, 2008, p. 1–8.